Computational Materials Science 169 (2019) 109143

Contents lists available at ScienceDirect

Computational Materials Science

journal homepage: www.elsevier.com/locate/commatsci

# Reactive molecular dynamics simulation of the amorphous carbon growth: Effect of the carbon triple bonds

Xiaowei Li[a,b,*], Hiroshi Mizuseki[a], Sung Jin Pai[a], Kwang-Ryeol Lee[a,*]

[a] Computational Science Center, Korea Institute of Science and Technology, Seoul 136-791, Republic of Korea
[b] Key Laboratory of Marine Materials and Related Technologies, Zhejiang Key Laboratory of Marine Materials and Protective Technologies, Ningbo Institute of Materials Technology and Engineering, Chinese Academy of Sciences, Ningbo 315201, PR China

ARTICLE INFO

*Keywords:*
Triple bond
Dynamic growth
Amorphous carbon
Molecular dynamics
ReaxFF potential

ABSTRACT

The growth behavior of amorphous carbon (a-C) film was studied by reactive molecular dynamics simulation using the atom-by-atom deposition approach. Various reactive force field (ReaxFF) models were compared in terms of the structural properties of the resulting a-C films. By linking the structural properties of the film with the difference in the parameter sets of the ReaxFF models, we reveal that the carbon triple bond stabilization energy in the ReaxFF model, $\nu_{trip}$, significantly affects the growth dynamics and structural evolution of the simulated a-C films. When the negative $\nu_{trip}$ value is too high, the generation of a large number of C—C dimers and triple bond-terminated chain structures induces an etching-like process. In contrast, too small negative value results in an overestimation of both the formation energy for C—C dimers and the bonding energy for terminal triple bonds. By *ab initio* calculation of the triple bond and comparing it with the molecular static calculation using the ReaxFF models, we tailored the $\nu_{trip}$ value to −13.34 kcal/mole, and the simulated a-C film has an atomic structure comparable with the existing experimental and theoretical results.

## 1. Introduction

Amorphous carbon (a-C) films have attracted much attention in the scientific and engineering fields because of their excellent mechanical, tribological, optical, and chemical-resistant properties [1–4]. In particular, the superior anti-friction and wear resistance behaviors make a-C a strong candidate as a solid lubricant against the mechanical damage of moving components, such as cutting tools, automobile engines, and aerospace components [5–8]. Due to the experimental limitations in precisely characterizing the complicated evolution of a-C structure and understanding the fundamental mechanisms, molecular dynamics (MD) simulations [9–16], especially empirical MD simulations [9–11,14–16], have been employed to fabricate various a-C structures in large scale and investigate the relationship between the structure and the properties.

In the empirical MD simulation, the reliable description of interatomic interactions is strongly and solely dependent on the empirical interatomic potential, which plays a crucial role in the accurate simulation of the a-C structure [17–19]. More than ten potentials have been proposed since 1988, including Tersoff [20,21], REBO [22], AIREBO [23], reactive force field interatomic potential (ReaxFF) [24], environment-dependent interaction potential [25], charge-optimized many-body potential [26], and long-range carbon bond-order potential [27]. Among them, ReaxFF, an empirical bond-order potential developed by van Duin et al. [24], has received significant attention recently because it bridges the gap between the quantum chemical and empirical force fields, enabling the simulations to more accurately describe the process with chemical reactions using significantly fewer computational resources. In addition, it is a transferable potential, in which all parameter sets are based on the same functional form, allowing its application to the fields of combustion, catalysis, material failure, high-energy materials, tribology, biomaterials, batteries, and fuel cells.

To date, ReaxFF MD (RMD) has been extensively adopted to study the chemical reactions and structural variations of a-C in the atomic scale [15,18,28]. By comparing with the Tersoff and REBO potentials, Li et al. [18] revealed that the ReaxFF potential is capable of describing the a-C at densities smaller than 2.6 g/cm$^3$. Li et al. [28] investigated the graphitization of a-C under different simulation parameters and found that both the ReaxFF potential sets, separately reported by Chenoweth [29] and Srinivasan [30], were appropriate for simulating the growth of graphitic structures. Jensen et al. [31] also reported that ReaxFF by Srinivasan [30] produced the reliable mechanical properties of a-C, which compared favorably to the experimental results. Lotfi et al. [32] performed ReaxFF-based simulations to study the

* Corresponding authors at: Computational Science Center, Korea Institute of Science and Technology, Seoul 136-791, Republic of Korea (X. Li).
*E-mail addresses:* lixw0826@gmail.com (X. Li), krlee@kist.re.kr (K.-R. Lee).

https://doi.org/10.1016/j.commatsci.2019.109143
Received 13 May 2019; Received in revised form 12 July 2019; Accepted 14 July 2019

degradation chemistry of a perfluoropolyether lubricant in the presence of different a-C structures. However, previous RMD studies fabricated the a-C structure using the liquid-quenching method with fixed system volume [18,28,31,32]. Although this approach could produce the similar hybridized structures and densities of a-C to those achieved in the experiments [32], it deviates from the fully dynamic evolution of a-C growth in the experiments, including adsorption, implantation, and rebounding of incident C atoms [33]. Most importantly, the ReaxFF potential is composed of many energy terms and parameters (e.g., charge polarization, over- or under-coordination, terminal triple bond, and torsion), and a variety of ReaxFF parameter sets have been reported for carbon-based system, but it is unclear which parameter set should be used for simulating the a-C growth behavior.

In the present work, we performed RMD simulations to determine the dependence of a-C films on ReaxFF parameters and adopted the atom-by-atom deposition method to simulate the dynamic growth process of a-C films, although it is a very time-consuming operation. The ReaxFF potentials developed by Srinivasan (ReaxFF-Srinivasan) [30], Tavazza (ReaxFF-Tavazza) [34], and Han (ReaxFF-Han) [35] were selected, respectively, to simulate the a-C film growth. Among them, ReaxFF-Srinivasan has been validated to accurately evaluate the mechanical properties of carbon-based phases, including diamond, graphene, carbon nanotubes, and bulk amorphous carbon; ReaxFF-Tavazza is a revised version of ReaxFF-Srinivasan, which well describes the diamond tip-substrate interaction during nanoindentation; ReaxFF-Han is a randomly selected one for comparison with the ReaxFF-Srinivasan and ReaxFF-Tavazza potentials. A parametric study was performed by monitoring the responses of a-C configurations using various levels of ReaxFF parameter sets. By performing an in-depth analysis of the density, the hybridized structure, and the atomic bond structure, we revealed that the choice of the parameter set, especially the terminal triple bond energy parameter, had a significant effect on the simulation results. This finding not only further promotes the development and application of the ReaxFF potential, but also provides an accurate description of the structure-property relationship and potential mechanism for complicated carbon-based systems.

## 2. Computational methods

The large-scale atomic/molecular massively parallel simulator (LAMMPS) [36] was used to carry out the RMD simulations of a-C growth, which is a classical and open-source MD simulation code to run efficiently on parallel computers and developed by Sandia National Laboratories. Fig. 1 shows the three-dimensional (3D) model used in the calculations based on the previous studies [17]. A diamond (0 0 1) single crystal served as a substrate, consisting of 1856 carbon atoms and being divided into 29 atomic layers. A three-layer model was applied to the substrate, including a fixed layer (red region in Fig. 1), the thermostatic layer (blue region in Fig. 1), and the free layer (remaining region in Fig. 1). Among them, the fixed layer was used to mimic the semi-infinite substrate, the thermostatic layer was maintained at 300 K using the microcanonical (*NVE*) ensemble with a Berendsen thermostat [37] to provide a thermal reservoir for the simulated system, and the others were completely unconstrained to simulate the structural evolution during the deposition process. The incident carbon atoms were introduced at the position of 50 Å above the substrate surface at a random {*x*, *y*} position, a time step of 0.25 fs was used, and the periodic boundary condition was applied along the *x* and *y* directions.

Three potential parameter sets, including ReaxFF-Srinivasan [30], ReaxFF-Tavazza [34], and ReaxFF-Han [35], were used to study their effects on the a-C film growth, which were provided in the Supporting Information S1–S3. AIREBO potential [23] was also considered for comparison. Before the deposition process, the substrate was first equilibrated at 300 K for 100 ps using *NVE* ensemble. Then, 1740 carbon atoms with a normal incident angle and an incident energy of 70 eV/atom were deposited onto the substrate individually [17]; the time interval between the sequential carbon atom depositions was 10 ps, which was sufficient to relax the atomic structure induced by the bombardment of energetic incident carbon [33]. Next, the system was relaxed at 300 K for 1250 ps to obtain the final structure for analyzing the structural properties. The cutoff distance of 1.85 Å was used to evaluate the coordination number of C atoms. More details can be found in our previous study [17].

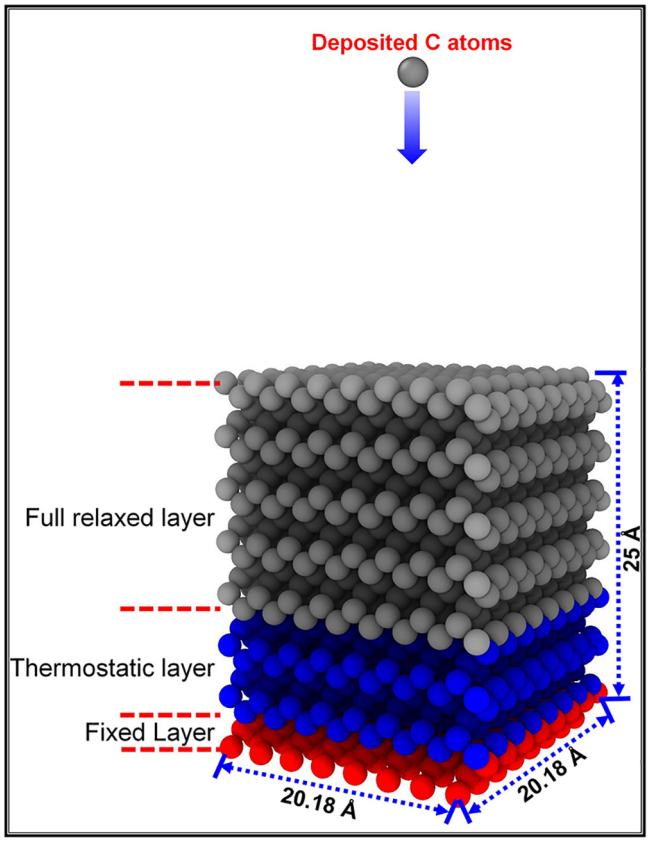


**Fig. 1.** Deposition model used in the calculations.

## 3. Results and discussion

### 3.1. Results

Fig. 2a shows the final morphology of the deposited film, obtained using ReaxFF-Srinivasan, ReaxFF-Tavazza, and ReaxFF-Han potentials separately. After the deposition process, an a-C film with a thickness of 64 Å is achieved for ReaxFF-Tavazza. However, the film thickness significantly decreases to 32 Å for ReaxFF-Srinivasan and 30 Å for ReaxFF-Han owing to aggravated etching. Different surface states and hybridized structures are observed for each potential. Since the incident energy of deposited carbon atoms (70 eV/atom) is much higher than the cohesive energy of diamond (7.6–7.7 eV/atom) [38], the incident C atoms easily etch or penetrate the diamond substrate, leading to the intermixing of deposited and substrate C atoms for a-C dynamic growth (inset of Fig. 2a).

Further analysis of the thickness dependence of the structural properties (Fig. 2b) shows that the film obtained using ReaxFF-Tavazza is also divided into three regions, including interfacial intermixing region (yellow background), steady-state growth region (light blue background), and surface transition region (gray background), similar to our previous study with AIREBO [17]. The thickness of the surface region obtained using ReaxFF-Tavazza is much wider than that using AIREBO due to the existence of many dangling bonds and linear chains. There is no steady-state growth region for the film obtained using

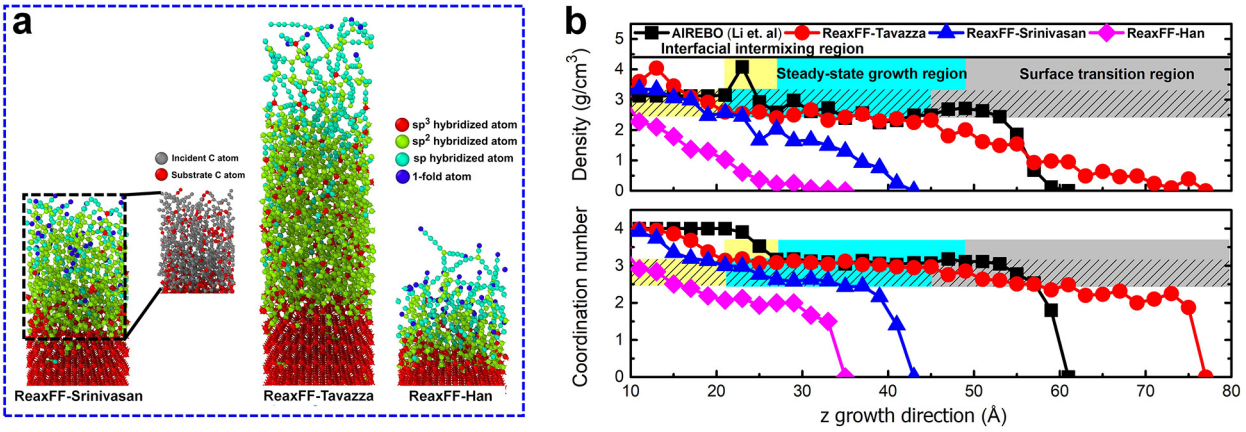


**Fig. 2.** (a) Final morphologies of deposited films obtained using ReaxFF-Srinivasan, ReaxFF-Tavazza, and ReaxFF-Han potentials, respectively, in which the dark blue, light blue, green, and red colors correspond to 1-, 2-, 3-, and 4-fold hybridized C atoms, and the inset is the corresponding morphology presented according to different atom types. (b) Thickness dependence of density and coordination number for the films obtained using ReaxFF-Srinivasan, ReaxFF-Tavazza, and ReaxFF-Han potentials. The results using AIREBO are also considered for comparison [17].

**Table 1**
Density and hybridized structure in steady-state growth region using ReaxFF-Tavazza and AIREBO potentials.

| Potentials | Density/g/cm$^3$ | sp$^3$/at.% | sp$^2$/at.% | sp/at.% |
|---|---|---|---|---|
| AIREBO | 2.56 | 11.4 | 86.9 | 1.7 |
| ReaxFF-Tavazza | 2.45 | 13.8 | 78.7 | 7.4 |

ReaxFF-Srinivasan and ReaxFF-Han; on the contrary, the density and coordination number with film thickness gradually decrease to 0, suggesting the significant effect of parameter sets on the dynamic growth of a-C films. Furthermore, in the steady state growth region of the films obtained using ReaxFF-Tavazza, the constant density and coordination numbers are achieved, which are normally adopted to represent the structural properties of deposited a-C films. Table 1 illustrates the density and hybridized structures (sp$^3$, sp$^2$, and sp) calculated for the steady-state growth region using ReaxFF-Tavazza, which are comparable to those calculated using AIREBO [17].

In order to explain the different dynamic growth behaviors of a-C films shown in Fig. 2, the parameter sets from three ReaxFF potentials are compared. ReaxFF-Han shows a great difference in parameter sets from ReaxFF-Srinivasan and ReaxFF-Tavazza. Consequently, the following comparative study mainly focuses on ReaxFF-Srinivasan and ReaxFF-Tavazza potentials to rapidly identify the key parameter factors, and the differences between these two potentials originate from the charge polarization, under-coordination energy, and terminal triple bond stabilization terms (Table 2).

**Table 2**
Difference in parameter sets between the ReaxFF-Tavazza and ReaxFF-Srinivasan potentials, including charge polarization, under-coordination energy, and terminal triple bond stabilization terms.

| Potentials | Charge polarization | | | Under-coordination |
|---|---|---|---|---|
| | $\gamma$/Å | $\chi$/eV | $\eta$/eV | $E_{under}$/kcal/mole |
| ReaxFF-Tavazza | 0.8485 | 4.8446 | 7.0000 | 30.0000 |
| ReaxFF-Srinivasan | 0.7920 | 6.7897 | 6.0000 | 27.5134 |

| Potentials | Terminal triple bond stabilization | | | |
|---|---|---|---|---|
| | $\nu_{trip}$/kcal/mole | $\lambda_4$ | $\lambda_5$ | $\lambda_8$ |
| ReaxFF-Tavazza | −63.5000 | 1.7224 | 6.8702 | 4.60 |
| ReaxFF-Srinivasan | −101.4874 | 1.9940 | 2.3157 | 4.60 |

### 3.1.1. Charge polarization term

ReaxFF is capable of calculating the polarization of charges within molecules, which is reached by using electronegativity and hardness parameters for each element in the system. This polarization is calculated as follows [39]:

$$\frac{\partial E}{\partial q_n} = \chi_n + 2\cdot q_n\cdot\eta_n + C\cdot\sum_{j=1}^{n}\frac{q_j}{\left\{r_{nj}^3+\left(1/\gamma_{nj}\right)^3\right\}^{1/3}\left\{r_{nj}^3+\left(1/\gamma_{nj}\right)^3\right\}}, \quad (1)$$

$$\sum_{i=1}^{n} q_i = 0, \quad (2)$$

where $\chi_n$ and $\eta_n$ are the electronegativity and hardness of element $n$, respectively; $\gamma_{nj}$ is the shielding parameter between the atoms $n$ and $j$; $q_n$ is the atom charge and $r$ is the interatomic distance. This method is based on the Electron Equilibration Method [40], which is similar to the QEq method [41]; the charge values are determined for each time step of the simulation and dependent on the geometry of the system.

### 3.1.2. Under-coordination energy term

Normally, the bond order is 4 for C, but the change in the distance between the two atoms may lead to over-coordinated or under-coordinated cases. For an under-coordinated atom ($\Delta_i < 0$), the energy contribution for the resonance of π-electrons between the attached under-coordinated atomic centers, $E_{under}$, is considered by the ReaxFF potential [24]. In Eqs. (3)–(5), $E_{under}$ is only important if the bonds between the under-coordinated atom $i$ and its under-coordinated neighbors $j$ partly have the π-bond character.

$$\Delta_i = \sum_{j=1}^{nbond} BO_{ij} - Val_i, \quad (3)$$

$$E_{under} = -p_{under}\cdot\frac{1-\exp(\lambda_7\cdot\Delta_i)}{1+\exp(-\lambda_8\cdot\Delta_i)}\cdot f_6(BO_{ij,\pi},\Delta_j), \quad (4)$$

$$f_6(BO_{ij,\pi},\Delta_j) = \frac{1}{1+\lambda_9\cdot\exp\left(\lambda_{10}\cdot\sum_{j=1}^{neighbors(i)}\Delta_j\cdot BO_{ij,\pi}\right)}, \quad (5)$$

where $\Delta_i$ is the deviation degree of the sum of the corrected bond orders around an atomic center from its valency Vali (Vali = 4 for carbon).

### 3.1.3. Terminal triple bond stabilization term

Strachan et al. [42] reported that for a system at equilibrium, the triple bond usually had a bond order of about 2.7, suggesting the incompletely filled valence band. For internal triple bonds, this loss of

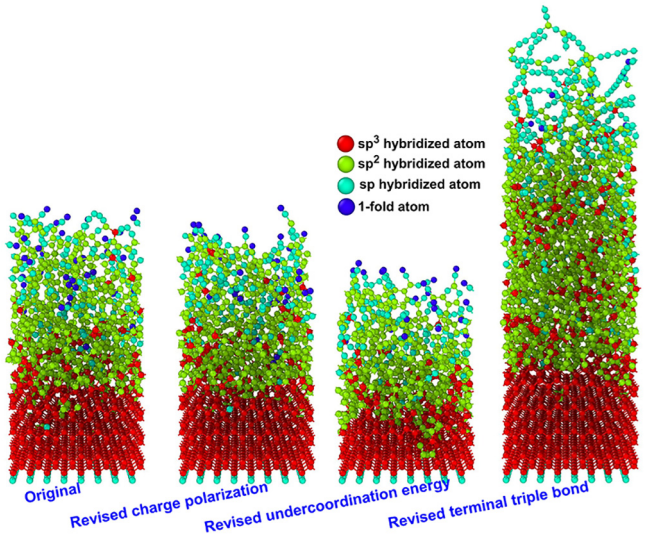


**Fig. 3.** Final morphologies of the deposited film obtained using ReaxFF-Srinivasan potentials with revised change polarization, under-coordination energy, and terminal triple bond terms. For comparison, the original case is also presented.

bonding is settled by introducing the under-coordination term, but this approach considers too little stability for terminal triple bonds. Hence, the terminal triple bond stabilization term, given by Eq. (6), is used to compensate the additional stabilization of terminal triple bonds.

$$E_{trip} = \upsilon_{trip}\exp[-\lambda_8(BO_{ij} - 2.5)^2] \times \frac{1}{1 + 25\exp[\lambda_5(\Delta_i + \Delta_j)]} \times [\exp[-\lambda_4(SBO_i - BO_{ij})] + \exp[-\lambda_4(SBO_j - BO_{ij})]], \quad (6)$$

where $SBO_i$ and $SBO_j$ are the sum of the bond orders around atoms $i$ and $j$; $\Delta_i$ and $\Delta_j$ describe the over-coordination in atoms $i$ and $j$ by subtracting the valency of these atoms from $SBO_i$ and $SBO_j$; $\lambda_4$, $\lambda_5$, and $\lambda_8$ are the atom parameters for bond order; $\upsilon_{trip}$ is the triple bond stabilization energy.

According to the ReaxFF-Tavazza potential, the parameters including the terminal triple bond parameters, charge polarization, and under-coordination terms in ReaxFF-Srinivasan are revised separately to explore the dependence of the a-C dynamic growth on each parameter term. Fig. 3 shows the final morphologies obtained using revised ReaxFF-Srinivasan potentials. When the charge polarization and under-coordination energy terms are revised separately to the values in the ReaxFF-Tavazza potential, the phenomenon is similar to the case using original ReaxFF-Srinivasan, which exhibits an etching-like process rather than the steady-state growth of the a-C film. This suggests that the parameters from both the under-coordination energy and charge polarization terms have little effect on the dynamic growth of a-C. However, the case with revised terminal triple bond terms shows an a-C film with a total thickness of ~64 Å, which is close to that obtained using the ReaxFF-Tavazza potential and the steady-state growth of a-C can be achieved (see Fig. S1 of Supporting Information), implying the significant role of this term in the a-C structure.

Using the steady-state growth region defined in Fig. S1 of Supporting Information, the structural property of the a-C film obtained using ReaxFF-Srinivasan with the revised terminal triple bond term is further quantified (Fig. 4). The results using AIREBO and ReaxFF-Tavazza (Table 1) potentials are also included for comparison. As the potential changes from AIREBO to ReaxFF-Tavazza and revised ReaxFF-Srinivasan potentials, the density (Fig. 4a) and the hybridized structure (Fig. 4b) display similar values. Fig. 4c further compares the density-$sp^3$ fraction relationship between the present work and the experimental results by Fallon et al. [43] and the ab initio simulation results by Koivusaari [44]. Although the empirical simulations in this study produce lower values than the experimental reports in Fallon et al. [43], the relationship between the $sp^3$ fraction and density obtained by the simulations using revised ReaxFF-Srinivasan or ReaxFF-Tavazza potentials agrees well with that of the *ab initio* simulations [44] where the a-C film was fabricated using the liquid-quenching method and that of the MD simulation using the AIREBO potential [17]. The experimental results [43] in Fig. 4c can be debated because they are based on a hypothetical spectroscopic analysis to quantify the $sp^3$ bond fraction [45,46].

Fig. 4d shows the radial distribution function (RDF) for each case, which is an effective tool to rapidly evaluate the variations in the atomic bond structure of a-C films [17]. All RDF functions exhibit the typical amorphous character; i.e., the long-range disorder with the short-range order. Compared with the RDF spectra using AIREBO and ReaxFF-Tavazza potentials, there are no obvious deviations in the first and second nearest neighbor peak positions as the ReaxFF-Srinivasan potential with the revised terminal triple bond term is used. Because the first nearest peak position is related to the bond length and the second nearest peak position is related to both the bond length and bond angle, the change in the RDF spectra suggests that a similar structure is obtained for each potential. Hence, these three potentials (AIREBO, ReaxFF-Tavazza, and ReaxFF-Srinivasan with the revised terminal triple bond term) show similar structural properties of a-C films.

Figs. 3 and 4 demonstrate that as $\lambda_4$, $\lambda_5$, $\lambda_8$, and $\upsilon_{trip}$ in the terminal triple bond term of ReaxFF-Srinivasan are modified to the corresponding values in ReaxFF-Tavazza (Table 2), the steady-state dynamic growth of a-C can be achieved, and the structural properties are also comparable to those obtained from MD using AIREBO [17] and the experimental observation. While $\lambda_4$, $\lambda_5$, and $\lambda_8$ are related to the bond order, the $\upsilon_{trip}$ parameter directly contributes to the triple bond stabilization term. Table 2 shows that the difference in terminal triple bond parameters between the ReaxFF-Tavazza and original ReaxFF-Srinivasan potentials mainly results from the $\upsilon_{trip}$ value, which is −101.4874 kcal/mole for original ReaxFF-Srinivasan and −63.5 kcal/mole for ReaxFF-Tavazza, respectively. To confirm the role of the $\upsilon_{trip}$ value on a-C growth, we further modify $\upsilon_{trip}$ from −63.5 to −70.5044 kcal/mole used in the ReaxFF-Han potential [35]. We observe the steady-state growth region with a reduced width compared to the case at −63.5 kcal/mole (see Fig. S2 of Supporting Information), indicating that the $\upsilon_{trip}$ value in the terminal triple bond term determines whether the steady-state growth of a-C can be achieved.

### 3.2. Discussion

In order to understand the effect of the terminal triple bond term, especially the $\upsilon_{trip}$ value, on the dynamic growth of a-C films, Fig. 5 presents the evolution of a-C morphologies during the deposition process when different $\upsilon_{trip}$ values are used. As the $\upsilon_{trip}$ value is −101.4874 kcal/mole (Fig. 5a), there is no steady-state growth region due to the etching-like process (Fig. 2b), but many C—C dimers and chain structures are generated during the entire process and dispersed in the surface and bulk carbon networks (see Supporting Video S1). However, as the $\upsilon_{trip}$ increases to −63.5 kcal/mole (Fig. 5b), a steady-state growth region of a-C exists (Fig. 5), there are almost no C–C dimers, and only a few chains with terminated triple bonds are distributed at the surface region (Supporting Video S2).

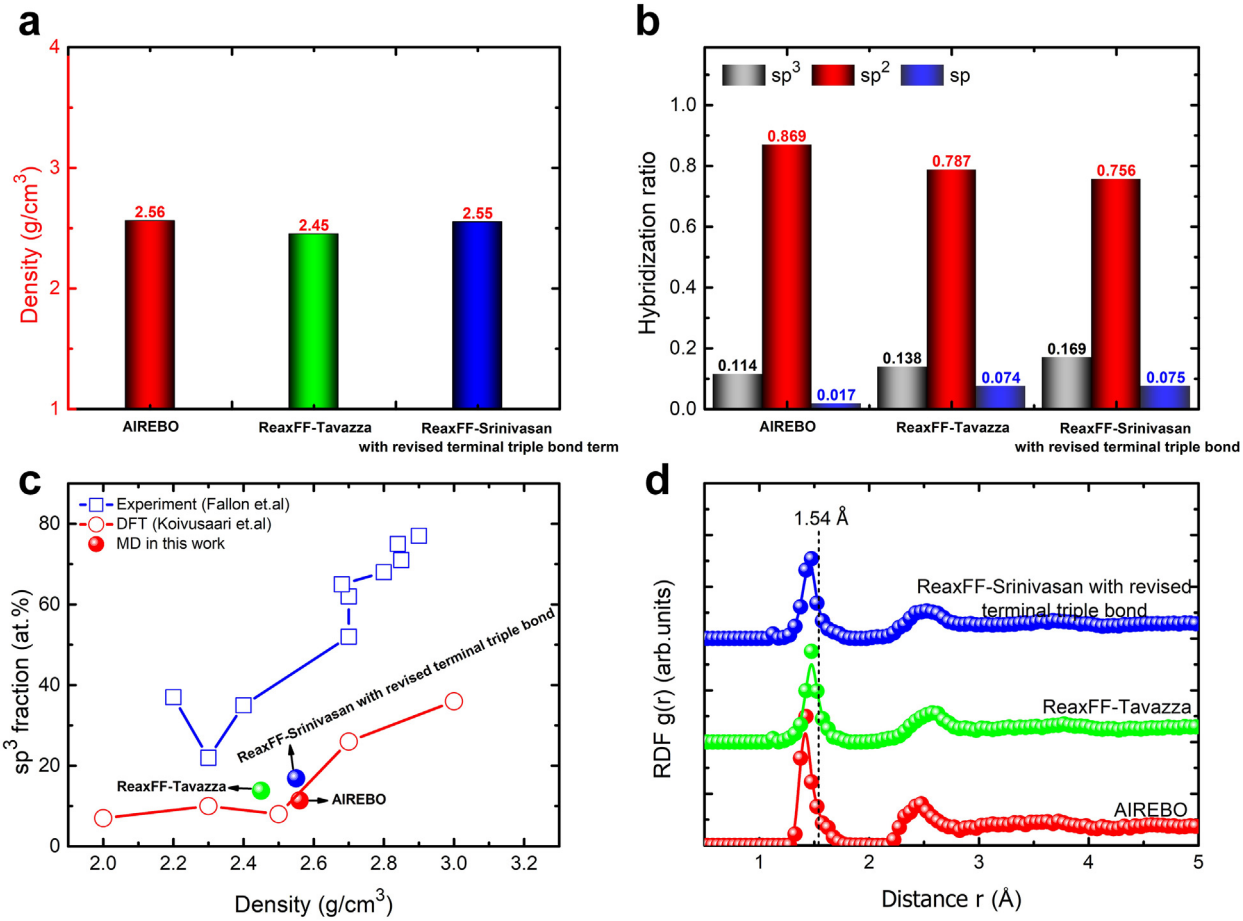


**Fig. 4.** Comparative results of a-C structures deposited with the atom-by-atom method using ReaxFF-Srinivasan with the revised terminal triple bond term, ReaxFF-Tavazza, and AIREBO potentials, respectively: (a) density; (b) hybridized structure ($sp^3$, $sp^2$, sp); (c) comparison of the $sp^3$ fractions and densities obtained in the present work with previous experimental [43] and calculated results [44]; (d) RDF spectra, in which the black vertical line represents the first nearest neighbor peak position of crystalline diamond.

**Video S1.**

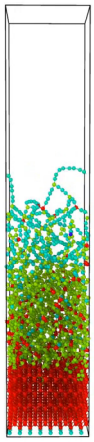

**Video S2.**

When the $\upsilon_{trip}$ value is −101.4874 kcal/mole in the ReaxFF-Srinivasan potential, the change in the local morphology of a-C during the deposition time ranged from 7,981,675 to 7,981,750 fs is illustrated in Fig. 6. There are many C—C dimers existed in bulk carbon networks, which tend to diffuse toward the a-C surface and are then evaporated from the system. Due to the interaction of surface chain structures, the C—C dimers are easily formed (Supporting Video S3), leading to the significant decrease in the number of deposited C atoms and the lack of steady-state growth. On the contrary, with the $\upsilon_{trip}$ value of −63.5 kcal/

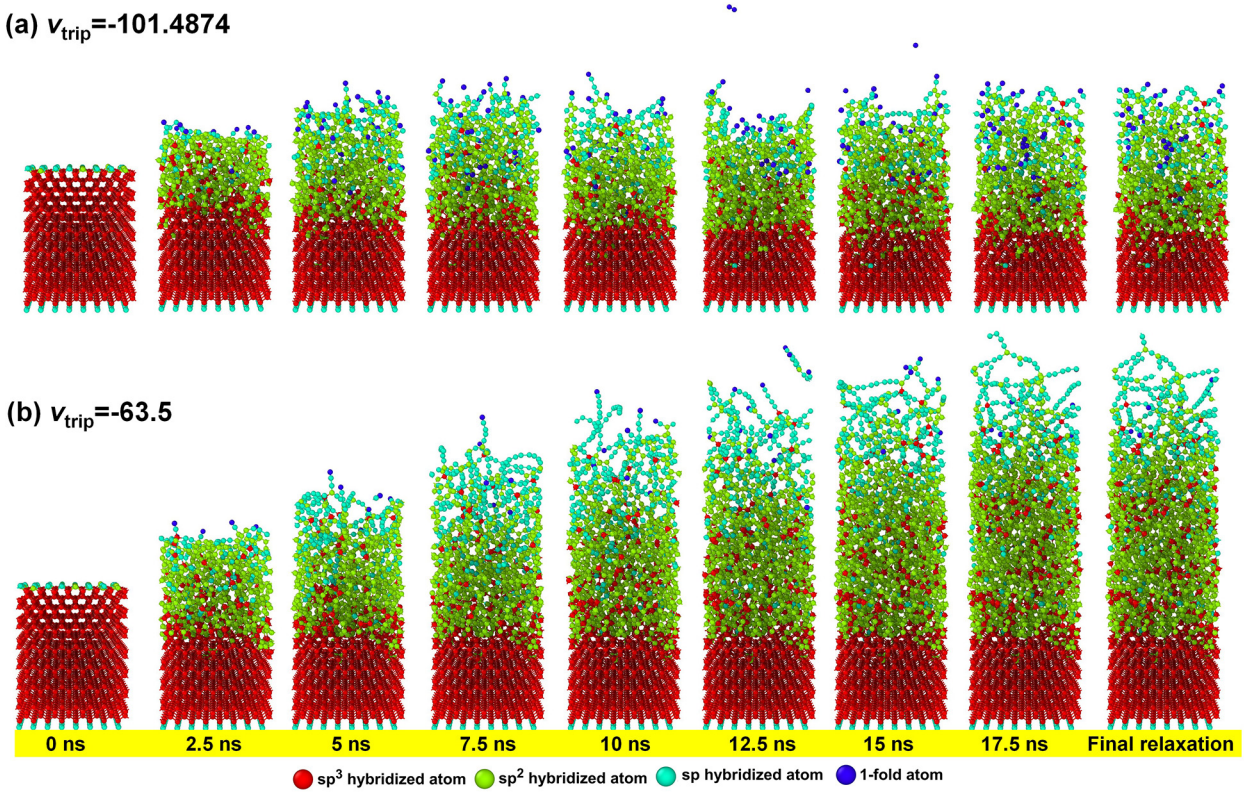


**Fig. 5.** Evolution of a-C morphologies during the deposition process when different $\upsilon_{trip}$ values of (a) −101.4874 and (b) −63.5 kcal/mole are used separately in the ReaxFF-Srinivasan potential.

mole (Fig. 7 and Supporting Video S4), the formation of triple bond-terminated structures and C—C dimers is inhibited effectively, contributing to the stable growth of a-C. Therefore, whether the stable growth of a-C can be achieved is strongly dependent on the formation of C—C dimers and triple bond-terminated structures, which are considerably affected by the $\upsilon_{trip}$ value.

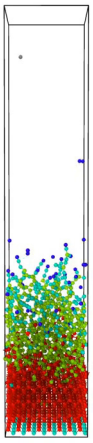

**Video S3.**

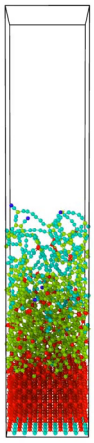

**Video S4.**

The formation energy of C—C dimers is calculated using ReaxFF-Srinivasan with different $\upsilon_{trip}$ values (Fig. 8a). With increasing the $\upsilon_{trip}$ value from −101.4874 to −63.5 kcal/mole, the formation energy increases gradually; when the $\upsilon_{trip}$ value is −101.4874 kcal/mole, the minimal formation energy is obtained. This indicates that compared to the case with the $\upsilon_{trip}$ value of −63.5 kcal/mole, the ReaxFF-Srinivasan with the $\upsilon_{trip}$ value of −101.4874 kcal/mole is more inclined to form the C—C dimers in order to further lower the total energy of the system (Figs. 5a and 6). For the triple bond-terminated chains, the bonding energy of each bond was also evaluated (Fig. 8b). The change in the $\upsilon_{trip}$ value of ReaxFF-Srinivasan potential has no effect on the bonding energies of single, double, and internal triple bonds. However, for the terminal triple bond, the bonding energy also increases gradually with the $\upsilon_{trip}$ value ranged from −101.4874 to −63.5 kcal/mole, suggesting the weakened bond stability and also accounting for the difference in

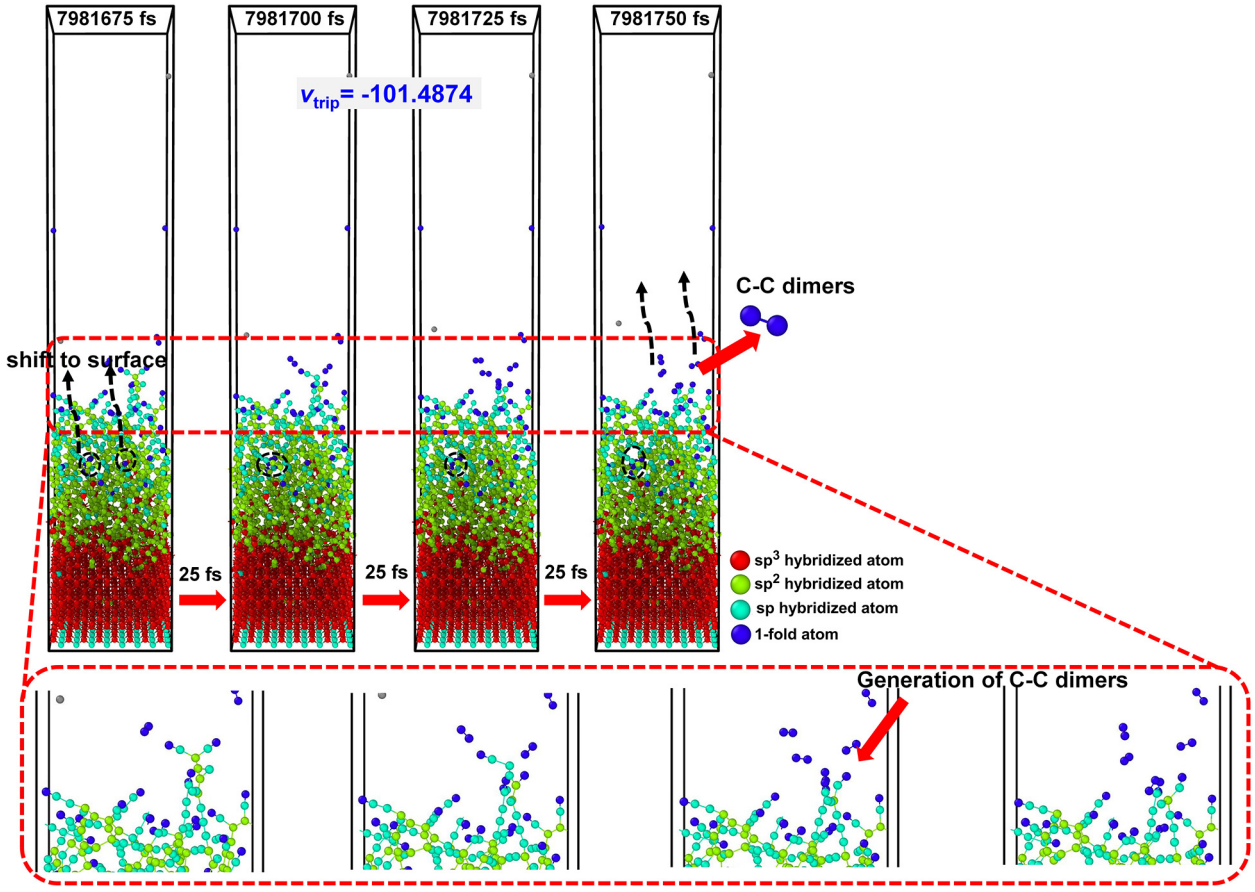


**Fig. 6.** Evolution of local morphology of a-C during the short range of deposition time from 7,981,675 to 7,981,750 fs when the $\upsilon_{trip}$ value is −101.4874 kcal/mole in ReaxFF-Srinivasan potential.

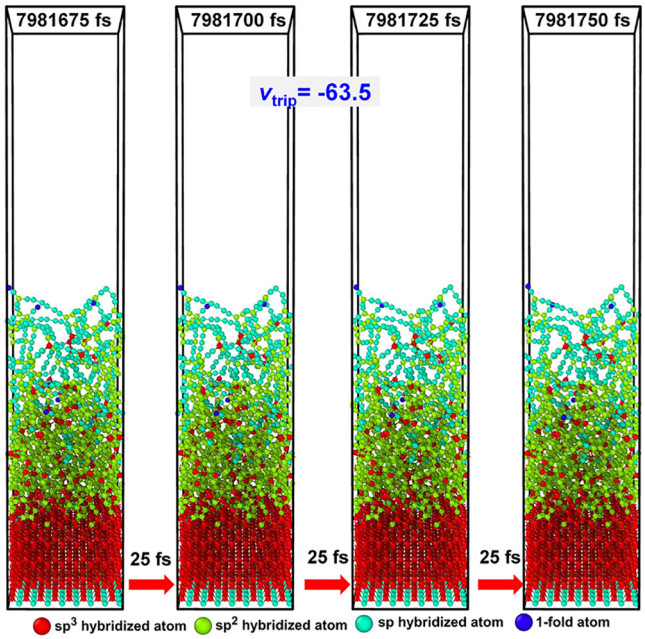


**Fig. 7.** Evolution of local morphology of a-C during the short range of deposition time from 7,981,675 to 7,981,750 fs when the $\upsilon_{trip}$ value is −63.5 kcal/mole in ReaxFF-Srinivasan potential.

the triple bond-terminated chain structures of the a-C surface (Figs. 6 and 7).

Note that increasing the $\upsilon_{trip}$ value from −101.4874 to −63.5 kcal/mole is favorable for the stable growth of a-C by the atom-by-atom approach, but Fig. 8b displays that for each case, the bonding energy of the terminal triple bond is still underestimated compared to that from the *ab initio* calculation. The computational details can be found in our previous work [47]. Hence, for an accurate $\upsilon_{trip}$ value in the ReaxFF-Srinivasan potential, Fig. 9 shows the relationship between the bonding energy of the terminal triple bond and the $\upsilon_{trip}$ value; when the $\upsilon_{trip}$ value is −13.34 kcal/mole, the obtained bonding energy using the ReaxFF-Srinivasan potential is equal to the *ab initio* result. The additional RMD simulation confirms that the a-C with increased thickness is achieved (Fig. 9b), and the problems with the triple bond-terminated chains and C−C dimers are effectively solved when the $\upsilon_{trip}$ value is −13.34 kcal/mole (Fig. 9b and Supporting Video S5), suggesting that this value is the most suitable one for the dynamic growth of a-C films. The full parameter sets for this potential can be found in Supporting Information S4.

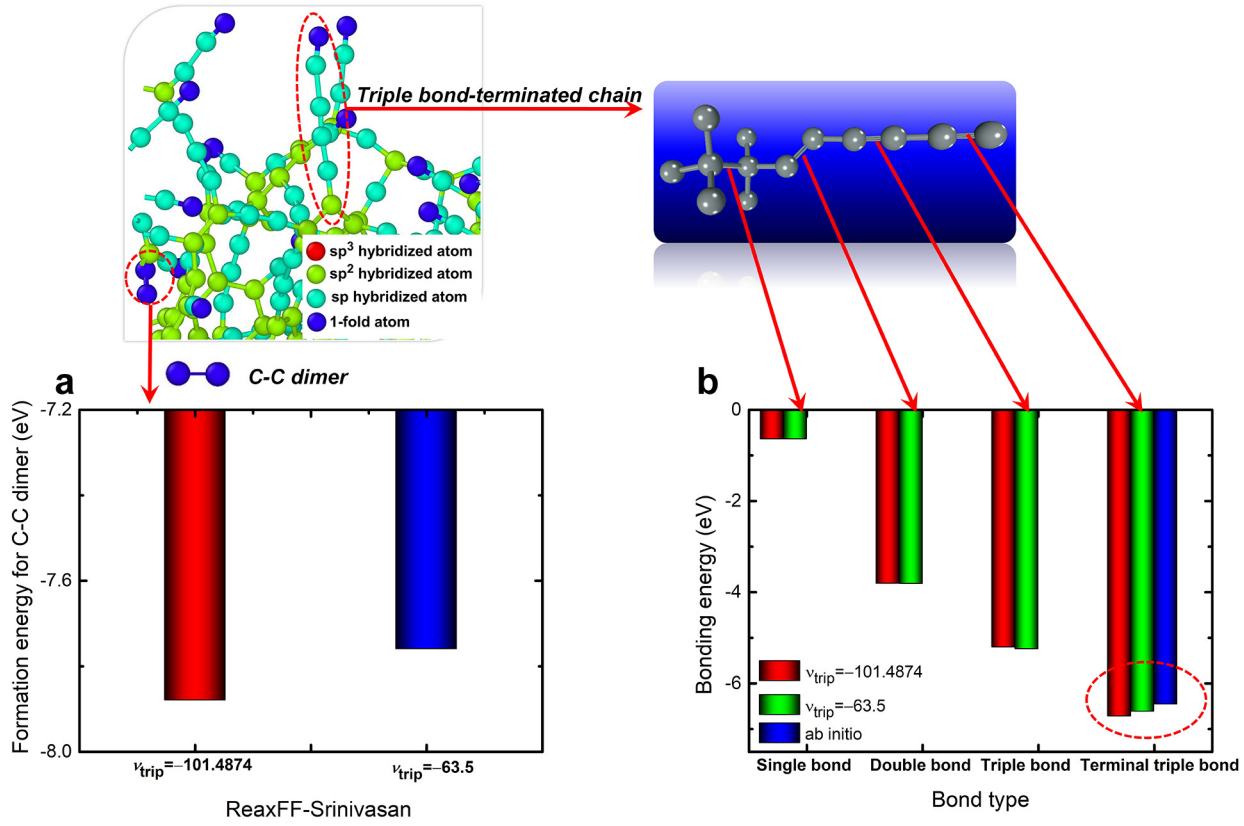


**Fig. 8.** Calculation of (a) formation energy of C—C dimers and (b) bonding energy of each bond in triple bond-terminated chain structure using ReaxFF-Srinivasan with $\upsilon_{trip}$ values of −101.4874 and −63.5 kcal/mole.

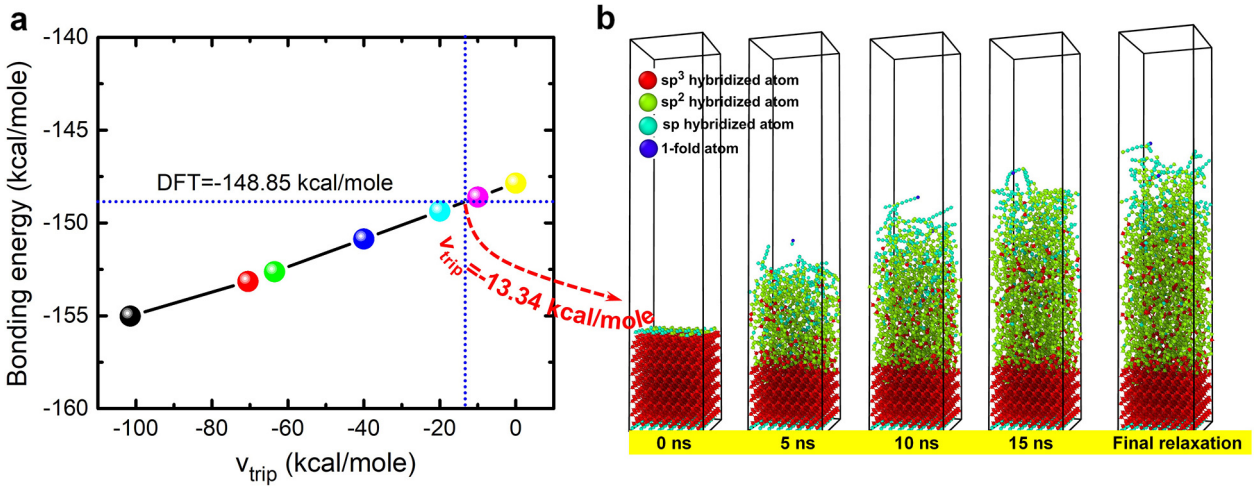


**Fig. 9. (a)** Relationship between the bonding energy of terminal triple bond and $\upsilon_{trip}$ value in ReaxFF-Srinivasan potential. (b) Morphologies of a-C films when the $\upsilon_{trip}$ value is −13.34 kcal/mole.

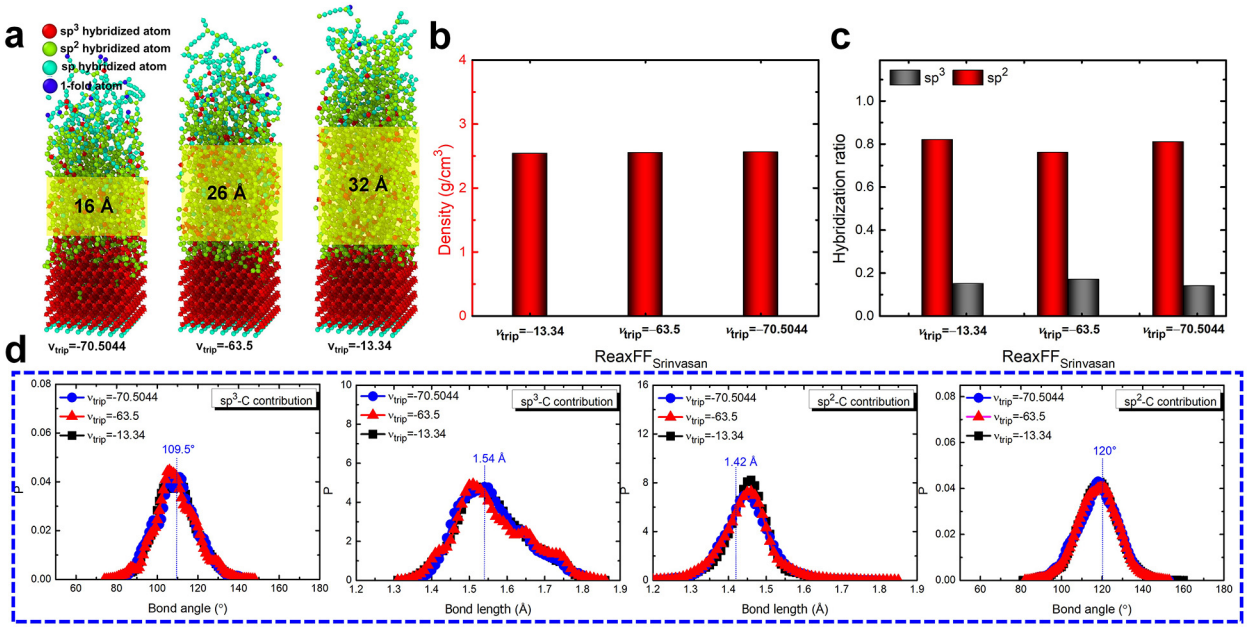


**Fig. 10.** Comparative results of a-C structures deposited with the atom-by-atom method using ReaxFF-Srinivasan with different $\upsilon_{trip}$ values (−70.5044, −63.5, and −13.34 kcal/mole): (a) final morphologies; (b) density; (c) hybridized structure ($sp^3$, $sp^2$, sp); (d) both the bond angle and length distributions from only $sp^3$ C or $sp^2$ C.

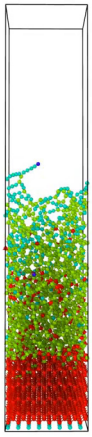

**Video S5.**

When the $\upsilon_{trip}$ value ranges from −70.5044 (Fig. S2 of Supporting Information) to −63.5 and −13.34 kcal/mole, the stable regions of a-C with thicknesses increasing from 16 to 26 and 32 Å are obtained (Fig. 10a). For the characterization of the potential effect of the $\upsilon_{trip}$ value on the structural properties of grown a-C, Fig. 10b and c present the comparative results including the density and the hybridized structure ($sp^3$, $sp^2$, sp) under different $\upsilon_{trip}$ values. The change in the $\upsilon_{trip}$ value has no effect on the density and hybridized values of grown a-C films. For more details on the atomic bond structure, both the bond angle and length distributions are further analyzed (Fig. 10d), in which the equilibrium bond angle and bond length of diamond are 109.5° and 1.54 Å, respectively, and those of graphite are 120° and 1.42 Å, respectively [17]. These values show that both the bond angle and the length distributions from only $sp^3$ C or $sp^2$ C are independent of the $\upsilon_{trip}$ values. Therefore, once the stable region is generated, further increasing the $\upsilon_{trip}$ value only changes the width of the stable region and it does not tailor the structural properties of a-C.

## 4. Conclusions

In this work, the RMD simulation was conducted to fabricate a-C films using the atom-by-atom deposition approach. The effect of ReaxFF parameter sets on the dynamic growth process of a-C was investigated. The following conclusions were obtained.

- Compared to the results using ReaxFF-Tavazza, the steady-state growth region was absent for the film obtained using the original ReaxFF-Srinivasan or ReaxFF-Han potential, suggesting the significant effect of parameter sets on the dynamic growth of a-C films.
- According to the ReaxFF-Tavazza potential, the charge polarization, under-coordination energy, and terminal triple bond stabilization terms in ReaxFF-Srinivasan were modified separately, revealing that only when the terminal triple bond stabilization term was revised, the steady-state growth of a-C could be achieved, and the obtained density and hybridized values were also comparable to those obtained using ReaxFF-Tavazza, AIREBO, and previous *ab initio* calculations.
- The difference in dynamic growth values was related to the $\upsilon_{trip}$ value in the terminal triple bond stabilization term. For the $\upsilon_{trip}$ value of −101.4874 kcal/mole, the C—C dimers and triple bond-terminated chains were easily formed due to the underestimation of both the formation energy of C—C dimers and the bonding energy of terminal triple bonds, leading to the significant decrease in the number of deposited C atoms and the lack of steady-state growth. However, this problem could be handled by increasing the $\upsilon_{trip}$ value to −63.5 kcal/mole, accounting for the existence of the stable growth region in a-C films. Both the *ab initio* and additional RMD results suggested that the $\upsilon_{trip}$ value of −13.34 kcal/mole should be used in the ReaxFF potential for the dynamic growth of a-C films.
- This study elucidates the importance of the terminal triple bond set of ReaxFF potential, especially the $\upsilon_{trip}$ value, in describing the complicated dynamic growth of a-C structures, and thus promotes the development and application of ReaxFF potential for carbon-based systems. In addition, compared to the AIREBO potential limited to the C/H systems, the ReaxFF potential shows greater potential to accurately simulate the physicochemical behaviors of

various carbon-contained systems.

## 5. Data availability

The authors declare that the data supporting the findings of this study are available within the paper and its Supporting information file.

## CRediT authorship contribution statement

**Xiaowei Li:** Conceptualization, Methodology, Software, Validation, Investigation, Writing - original draft, Writing - review & editing, Funding acquisition. **Hiroshi Mizuseki:** Conceptualization, Investigation, Writing - review & editing. **Sung Jin Pai:** Methodology, Investigation. **Kwang-Ryeol Lee:** Conceptualization, Methodology, Resources, Investigation, Writing - review & editing, Supervision, Funding acquisition.

## Conflicts of interest

The authors declare that they have no conflicts of interest to this work.

## Acknowledgments

This research was supported by the Korea Research Fellowship Program funded by the Ministry of Science and ICT through the National Research Foundation of Korea (2017H1D3A1A01055070), the Nano Materials Research Program through the Ministry of Science and IT Technology (NRF-2016M3A7B4025402), and the National Natural Science Foundation of China (51772307). The authors thank Prof. Liang Chen at Ningbo Institute of Materials Technology and Engineering, Chinese Academy of Sciences, for providing the supercomputer platform and productive discussion.

## Appendix A. Supplementary data

Deposition process of a-C using ReaxFF-Srinivasan with the $\upsilon_{trip}$ value of −101.4874 kcal/mole (Video S1). Deposition process of a-C using ReaxFF-Srinivasan with the $\upsilon_{trip}$ value of −63.5 kcal/mole (Video S2). Deposition process of a-C during the deposition time ranged from 7,981,675 to 7,981,750 fs using ReaxFF-Srinivasan with the $\upsilon_{trip}$ value of −101.4874 kcal/mole (Video S3). Deposition process of a-C during the deposition time ranged from 7,981,675 to 7,981,750 fs using ReaxFF-Srinivasan with the $\upsilon_{trip}$ value of −63.5 kcal/mole (Video S4). Deposition process of a-C using ReaxFF-Srinivasan with the $\upsilon_{trip}$ value of −13.34 kcal/mole (Video S5). Original parameter sets of ReaxFF-Srinivasan potential (S1). Original parameter sets of ReaxFF-Tavazza potential (S2). Original parameter sets of ReaxFF-Han potential (S3). Revised ReaxFF-Srinivasan potential with the $\upsilon_{trip}$ value of −13.34 kcal/mole (S4). Thickness dependence of density and coordination number for the films obtained using ReaxFF-Srinivasan potentials with revised terminal triple bond parameter, change polarization, and under-coordination energy terms. For comparison, the original case is also given (Fig. S1). Density and coordination number distributions along the film growth direction for the films obtained by ReaxFF-Srinivasan with different $\upsilon_{trip}$ values (−101.4874, −70.5044, and −63.5 kcal/mole), in which pink rectangle corresponds to the width of steady-state growth region of a-C when the $\upsilon_{trip}$ value is −63.5 kcal/mole, and blue rectangle corresponds to the width of steady-state growth region of a-C when the $\upsilon_{trip}$ value is −70.5044 kcal/mole (Fig. S2).Supplementary data to this article can be found online at https://doi.org/10.1016/j.commatsci.2019.109143.

## References

[1] X. Chen, C. Zhang, T. Kato, X. Yang, S. Wu, R. Wang, M. Nosaka, J. Luo, Evolution of tribo-induced interfacial nanostructures governing superlubricity in a-C: H and a-C:H: Si films, Nat. Commun. 8 (2017) 1675.
[2] J. Sun, Y. Zhang, Z. Lu, Q. Li, Q. Xue, S. Du, J. Pu, L. Wang, Superlubricity enabled by pressure-induced friction collapse, J. Phys. Chem. Lett. 9 (2018) 2554–2559.
[3] J. Huang, L. Wang, B. Liu, S. Wan, Q. Xue, In vitro evaluation of the tribological response of Mo-doped graphite-like carbon film in different biological media, ACS Appl. Mater. Interfaces 7 (2015) 2772–2783.
[4] L. Cui, Z. Lu, L. Wang, Probing the low-friction mechanism of diamond-like carbon by varying of sliding velocity and vacuum pressure, Carbon 66 (2014) 259–266.
[5] L. Wang, R. Zhang, U. Jansson, N. Nedfors, A near-wearless and extremely long lifetime amorphous carbon film under high vacuum, Sci. Rep. 5 (2015) 11119.
[6] Y. Wang, K. Gao, B. Zhang, Q. Wang, J. Zhang, Structure effects of $sp^2$-rich carbon films under super-low friction contact, Carbon 137 (2018) 49–56.
[7] X. Li, P. Guo, L. Sun, X. Zuo, D. Zhang, P. Ke, A. Wang, Ti/Al Co-doping induced residual stress reduction and bond structure evolution of amorphous carbon films: an experimental and ab initio study, Carbon 111 (2017) 467–475.
[8] Z. Cao, W. Zhao, Q. Liu, A. Liang, J. Zhang, Super-elasticity and ultralow friction of hydrogenated fullerene-like carbon films: associated with the size of graphene sheets, Adv. Mater. Interfaces 5 (2018) 1701303.
[9] Y.N. Chen, T.B. Ma, Z. Chen, Y.Z. Hu, H. Wang, Combined effects of structural transformation and hydrogen passivation on the frictional behaviors of hydrogenated amorphous carbon films, J. Phys. Chem. C 119 (2015) 16148–16155.
[10] T.B. Ma, L.F. Wang, Y.Z. Hu, X. Li, H. Wang, A shear localization mechanism for lubricity of amorphous carbon materials, Sci. Rep. 4 (2014) 3662.
[11] T.B. Ma, Y.Z. Hu, H. Wang, Molecular dynamics simulation of shear-induced graphitization of amorphous carbon films, Carbon 47 (2009) 1953–1957.
[12] Y. Wang, J. Xu, J. Zhang, Q. Chen, Y. Ootani, Y. Higuchi, N. Ozawa, J.M. Martin, K. Adachi, M. Kubo, Tribochemical reactions and graphitization of diamond-like carbon against alumina give volcano-type temperature dependence of friction coefficients: a tight-binding quantum chemical molecular dynamics simulation, Carbon 133 (2018) 350–357.
[13] Y. Wang, J. Xu, Y. Ootani, S. Bai, Y. Higuchi, N. Ozawa, K. Adachi, J.M. Martin, M. Kubo, Tight-binding quantum chemical molecular dynamics study on the friction and wear processes of diamond-like carbon coatings: effect of tensile stress, ACS Appl. Mater. Interfaces 9 (2017) 34396–34404.
[14] X. Li, P. Ke, K.R. Lee, A. Wang, Molecular dynamics simulation for the influence of incident angles of energetic carbon atoms on the structure and properties of diamond-like carbon films, Thin Solid Films 552 (2014) 136–140.
[15] X. Li, A. Wang, K.R. Lee, Mechanism of contact pressure-induced friction at the amorphous carbon/alpha olefin interface, NPJ Comput. Mater. 4 (2018) 53.
[16] G.T. Gao, P.T. Mikulski, J.A. Harrison, Molecular-scale tribology of amorphous carbon coatings: effects of film thickness, adhesion, and long-range interactions, J. Am. Chem. Soc. 124 (2002) 7202–7209.
[17] X. Li, A. Wang, K.R. Lee, Comparison of empirical potentials for calculating structural properties of amorphous carbon films by molecular dynamics simulation, Comput. Mater. Sci. 151 (2018) 246–254.
[18] L. Li, M. Xu, W. Song, A. Ovcharenko, G. Zhang, D. Jia, The effect of empirical potential functions on modeling of amorphous carbon using molecular dynamics method, Appl. Surf. Sci. 286 (2013) 287–297.
[19] M. Joe, M.W. Moon, K.R. Lee, Atomistic simulation of diamond-like carbon growth, Thin Solid Films 521 (2012) 239–244.
[20] J. Tersoff, New empirical approach for the structure and energy of covalent systems, Phys. Rev. B 37 (1988) 6991–7000.
[21] P. Erhart, K. Albe, Analytical potential for atomistic simulation of silicon, carbon, and silicon carbide, Phys. Rev. B 71 (2005) 035211.
[22] D.W. Brenner, O.A. Shenderova, J.A. Harrison, S.J. Stuart, B. Ni, S.B. Sinnott, A second-generation reactive empirical bond order (REBO) potential energy expression for hydrocarbons, J. Phys. Condens. Matter. 14 (2002) 783–802.
[23] J.A. Stuart, A.B. Tutein, J.A. Harrison, A reactive potential for hydrocarbons with intermolecular interactions, J. Chem. Phys. 112 (2000) 6472–6486.
[24] A.C.T. van Duin, S. Dasgupta, F. Lorant, W.A. Goddard III, ReaxFF: a reactive force field for hydrocarbons, J. Phys. Chem. A 105 (2001) 9396–9409.
[25] N.A. Marks, Thin film deposition of tetrahedral amorphous carbon: a molecular dynamics study, Diamond Relat. Mater. 14 (2005) 1223–1231.
[26] D. Zhang, M.R. Dutzer, T. Liang, A.F. Fonseca, Y. Wu, K.S. Walton, D.S. Sholl, A.H. Farmahini, S.K. Bhatia, S.B. Sinnott, Computational investigation on $CO_2$ adsorption in titanium carbide-derived carbons with residual titanium, Carbon 111 (2017) 741–751.
[27] J.H. Los, A. Fasolino, Intrinsic long-range bond-order potential for carbon: performance in Monte Carlo simulations of graphitization, Phys. Rev. B 68 (2003) 024107.
[28] K. Li, H. Zhang, G. Li, J. Zhang, M. Bouhadja, Z. Liu, A.A. Skelton, M. Barati, ReaxFF molecular dynamics simulation for the graphitization of amorphous carbon: a parametric study, J. Chem. Theory Comput. 14 (2018) 2322–2331.
[29] K. Chenoweth, A.C.T. van Duin, W.A. Goddard III, ReaxFF reactive force field for molecular dynamics simulations of hydrocarbon oxidation, J. Phys. Chem. A 112 (2008) 1040–1053.
[30] S.G. Srinivasan, A.C.T. van Duin, P. Ganesh, Development of a ReaxFF potential for carbon condensed phases and its application to the thermal fragmentation of a large fullerene, J. Phys. Chem. A 119 (2015) 571–580.
[31] B.D. Jensen, K.E. Wise, G.M. Odegard, Simulation of the elastic and ultimate tensile properties of diamond, graphene, carbon nanotubes, and amorphous carbon using a revised ReaxFF parametrization, J. Phys. Chem. A 119 (2015) 9710–9712.
[32] R. Lotfi, A.S.M. Jonayat, A.C.T. van Duin, M.M. Biswas, R. Hempstead, A reactive force field study on the interaction of lubricant with diamond-like carbon structures, J. Phys. Chem. C 120 (2016) 27443–27451.

[33] X. Li, P. Ke, H. Zheng, A. Wang, Structure properties and growth evolution of diamond-like carbon films with different incident energies: a molecular dynamics study, Appl. Surf. Sci. 273 (2013) 670–675.
[34] F. Tavazza, T.P. Senftle, C. Zou, C.A. Becker, A.C.T. van Duin, Molecular dynamics investigation of the effects of tip-substrate interactions during nanoindentation, J. Phys. Chem. C 119 (2015) 13580–13589.
[35] S.J. Pai, B.C. Yeo, S.S. Han, Development of the ReaxFF$_{CBN}$ reactive force field for the improved design of liquid CBN hydrogen storage materials, Phys. Chem. Chem. Phys. 18 (2016) 1818–1827.
[36] S. Plimpton, Fast parallel algorithms for short-range molecular dynamics, J. Comp. Phys. 117 (1995) 1–19.
[37] H.J.C. Berendsen, J.P.M. Postma, W.F. van Gunsteren, A. DiNola, J.R. Haak, Molecular dynamics with coupling to an external bath, J. Chem. Phys. 81 (1984) 3684–3690.
[38] T.B. Ma, Y.Z. Hu, H. Wang, X. Li, Microstructural and stress properties of ultrathin diamondlike carbon films during growth: molecular dynamics simulation, Phys. Rev. B 75 (2007) 035425.
[39] M.F. Russo Jr., A.C.T. van Duin, Atomistic-scale simulation of chemical reactions: bridging from quantum chemistry to engineering, Nucl. Instrum. Methods Phys. Res., Sect. B 269 (2011) 1549–1554.
[40] W.J. Mortier, S.K. Ghosh, S. Shankar, Electronegativity-equalization method for the calculation of atomic charges in molecules, J. Am. Chem. Soc. 108 (1986) 4315–4320.
[41] A.K. Rappe, W.A. Goddard III, Charge equilibration for molecular dynamics simulations, J. Phys. Chem. 95 (1991) 3358–3363.
[42] A. Strachan, E.M. Kober, A.C.T. van Duin, J. Oxgaard, W.A. Goddard III, Thermal decomposition of RDX from reactive molecular dynamics, J. Chem. Phys. 122 (2005) 054502.
[43] P.J. Fallon, V.S. Veerasamy, C.A. Davis, J. Robertson, G.A.J. Amaratunga, W.I. Milne, J. Koskinen, Properties of filtered-ion-beam-deposited diamondlike carbon as a function of ion energy, Phys. Rev. B 48 (1993) 4777–4782.
[44] K.J. Koivusaari, T.T. Rantala, S. Leppävuori, Calculated electronic density of states and structural properties of tetrahedral amorphous carbon, Diamond Relat. Mater. 9 (2000) 736–740.
[45] S. Kaciulis, Spectroscopy of carbon: from diamond to nitride films, Surf. Interface Anal. 44 (2012) 1155–1161.
[46] A. Fujimoto, Y. Yamada, M. Koinuma, S. Sato, Origin of $sp^3$C peaks in C1s photoelectron spectra of carbon materials, Anal. Chem. 88 (2016) 6110–6114.
[47] X. Li, D. Zhang, K.R. Lee, A. Wang, Effect of metal doping on structural characteristics of amorphous carbon system: a first-principles study, Thin Solid Films 607 (2016) 67–72.